Available online at www.sciencedirect.com
SCIENCE DIRECT
Catalysis Today 99 (2005) 89–98
CATALYSIS TODAY
www.elsevier.com/locate/cattod

A study of methane partial oxidation in annular reactor: activity of Rh/α-Al_2O_3 and Rh/ZrO_2 catalysts

Tiziana Bruno, Alessandra Beretta, Gianpiero Groppi, Massimo Roderi, Pio Forzatti*

Dipartimento di Chimica, Materiali e Ingegneria Chimica, Politecnico di Milano, Piazza Leonardo da Vinci 32, 20133 Milano, Italy

Available online 21 December 2004

Abstract

The activity of Rh/α-Al_2O_3 and Rh/ZrO_2 in CH_4 partial oxidation was investigated in an annular reactor, which operates at high space velocity, under kinetically controlled conditions and minimum temperature gradients along the catalyst bed. The effects of temperature, dilution, space velocity and CH_4/O_2 ratio were explored. Rh/α-Al_2O_3 provided higher H_2 yields than Rh/ZrO_2 at all conditions. Concerning the process kinetics, over Rh/α-Al_2O_3 an indirect-consecutive kinetic scheme for synthesis gas formation prevailed; the observed trends were in fact in line with the combined presence of methane total oxidation, methane reforming reactions and consecutive oxidations of H_2 and CO. Over Rh/ZrO_2 the additional contribution of a direct route to synthesis gas could not be excluded. The complexity of the reaction scheme seems associated with the existence of different active sites, whose concentration could be affected by metal-support interactions and Rh reconstruction during conditioning. Indeed, once exposed to the reaction atmosphere, the fresh catalysts showed an initial conditioning during which a specific activation of the high temperature routes (responsible for H_2 production) was observed.

Keywords: Methane partial oxidation; Rh/α-Al_2O_3 and Rh/ZrO_2 catalysts; Short contact time; Annular reactor

1. Introduction

The great potential of methane partial oxidation to CO/H_2 mixtures in catalytic short contact time reactors was first demonstrated by Schmidt and coworkers [1–3] and further confirmed by several authors [4–7]: very high yields to CO and H_2 were observed over noble metal-based catalysts, by running the process autothermally at few milliseconds contact times. The process is fast and exothermic, thus it is suitable to realize compact reformers with reduced thermal inertia, adequate to the development of a network for H_2 production and distribution to little-medium scale fuel cells [8]. Other proposed applications are the enhancement of gas turbine performances through the partial conversion of methane into a H_2 enriched stream prior to fuel lean combustion [9], the small scale production of reducing atmospheres for metallurgical treatments, the production of synthesis gas for fuelling solid oxide fuel cells [10].

It is generally agreed that Rh provides the best performances among other noble metals, in terms of H_2 yields, stability against volatilization, resistance to carbon deposition [11]. Minor attention has been given, instead, to the effect of support. Sintered ceramic foam monoliths or honeycombs have been mostly adopted for the autothermal partial oxidation of methane at high Rh loads (5–15%) [1–4]; a small effect of support was reported. Indeed, Bodke et al. [12], though they found that ZrO_2 monoliths gave higher H_2 selectivities than alumina monoliths, have related the results with the differences in mass transfer rates between different support geometries and morphologies. However, metal-support interactions are expected to become important in the case of well dispersed catalysts. A few works in the literature have addressed this issue, but results seem controversial. A general high activity of several Rh-supported catalysts was reported by Boucouvalas et al. [13] and kinetic data at low methane conversion were interpreted

* Corresponding author. Tel.: +39 0223993238; fax: +39 0223993318.
E-mail address: pio.forzatti@polimi.it (P. Forzatti).

0920-5861/$ – see front matter © 2004 Elsevier B.V. All rights reserved.
doi:10.1016/j.cattod.2004.09.027

in favor of an indirect scheme to H_2/CO formation. An important effect of the support on methane partial oxidation was found by Ruckenstein and Wang [14] who compared the performances of reducible (e.g. CeO_2, TiO_2, ZrO_2) and irreducible (γ-Al_2O_3, SiO_2, La_2O_3, MgO) oxides as Rh-supports (at 1% Rh loading). Irreducible oxides were found more active than reducible oxides; this was related to the relative ease of generation of metallic rhodium sites (proposed as active sites for syngas production) over irreducible supports. However, the catalyst performances were screened at fixed operating conditions (which could be not optimal for the different formulations); also, results could be biased by the effect of surface area, which varied considerably between the various supports. Majocchi et al. [15] verified that the use of hexaaluminates as Rh supports resulted in lower H_2 yields and lower stability than α-Al_2O_3, probably because of Rh inclusion. An important role of the support is inferred by the results of Wang et al. [16], who studied the mechanism of methane partial oxidation over a Rh/γ-Al_2O_3 catalyst; they proposed that the adsorption of water on the support acted as an oxygen source through inverse spillover of hydroxyls or H_2O to Rh sites.

It should be noted that an important prerequisite for the study of Rh-support interactions is the development of experimental tools for investigating the intrinsic kinetics of the process. This is a challenging objective in the case of methane partial oxidation, that operates under severe conditions and can in principle be affected by thermodynamic constraints, heat and mass transfer limitations, homogeneous reactions [17]. In previous works, the authors have verified the adequacy of a structured annular reactor for the kinetic investigation of methane partial oxidation over Rh-supported catalysts, and other ultra-fast catalytic reactions [18–21]. The annular reactor allows to control the extent of mass transfer limitations, to analyze the process far from the thermodynamic equilibrium constraints and to realize well controlled and accurately measured temperature conditions on the catalyst surface with minimum axial gradients. These highly desirable features provided the basis for addressing an on-going study on the effects that the catalytic material (nature of the support, Rh loading, methodology of preparation) exerts on synthesis gas formation.

In this work, a comparison is presented between the performances of Rh/α-Al_2O_3 and Rh/ZrO_2. The supports were selected from indications of the patent literature [22,23]; in particular, these materials are expected to guarantee thermal stability under reaction, resistance to thermal shocks and inertness to inclusion of Rh particles (an observed phenomenon in three-way catalysts, e.g. Rh/γ-Al_2O_3 [24]). The performances of the catalysts were studied over a wide range of operating conditions, thus extending the traditional standardized screening of materials to a more comprehensive investigation of the possible differences of the process kinetics on the two systems.

2. Experimental

2.1. Catalysts

A 0.5% Rh/α-Al_2O_3 and 0.5% Rh/ZrO_2 by weight were prepared by a grafting technique [25]. Before impregnation, the supports were calcined to reach the high temperature stable phases, which were verified by X-ray diffraction. A commercial γ-Al_2O_3 (Puralox Sba-150, Sasol) was calcined in air at 1100 °C for 10 h to obtain α-Al_2O_3 phase. The measured BET surface area was 12 m^2/g. A commercial ZrO_2 (XZO 881/04, Mel Chemicals) was calcined in air at 950 °C for 10 h; the monoclinic phase was thus obtained. The calcination temperature was selected in order to achieve a value of surface area of 15 m^2/g, comparable with that of α-Al_2O_3; the similar morphology was intended to better analyze the effective role of the chemical nature of the supports in the following impregnation step and in the activity tests.

The grafting procedure consisted in dissolving the necessary amount of $Rh_4(CO)_{12}$ (Strem Chemicals) in excess *n*-hexane (10^{-2} to 10^{-3} M) at room temperature, under magnetic stirring and inert N_2 atmosphere. The color of the solution was deep red, as typical of dissolved Rh-complexes. The powders of α-Al_2O_3 or ZrO_2 were added to the solution and kept under magnetic stirring and inert N_2 atmosphere, at room temperature. In the case of α-Al_2O_3, in about 0.5 h the reaction was complete and the solution turned transparent. In the case of ZrO_2, the reaction of the carbonyls with the support surface was much faster; the solution turned limpid almost instantaneously. Such higher reactivity of $Rh_4(CO)_{12}$ clusters was likely associated with the presence of surface hydroxyls in monoclinic zirconia, which is well known in [26]. Catalyst powders, slightly reddish, were then filtered under vacuum and dried at 60 °C for 2 h. Rh loadings were verified by atomic absorption analysis of the powder and the exhaust solution.

The catalysts were tested in the form of thin layers, deposited onto ceramic tubular supports, obtained according to the following procedure. After drying, the catalyst powders were dispersed in HNO_3 and water and the obtained slurry was ball milled with zirconia spheres for 24 h. After deposition of a layer of primer (Disperal®, Sasol), the ceramic tubes were dip coated in the slurry and then dried at 280 °C. Well adherent catalyst layers (5–6 mg, 10–20 μm thin, 22 mm long) were obtained. Operating conditions of the single procedure steps are summarized in Table 1. Atomic absorption analysis of the dried slurry powder confirmed that no loss of Rh had occurred before deposition.

Measurements of metal dispersion were carried out on fresh and aged catalysts by pulse H_2 chemisorption in a Thermo Electron Corporation TPD/R/O 1100 Catalytic Surface Analyzer. After pre-treating 150 mg of sample at 500 °C for 1 h in flowing pure H_2, analyses were performed at 273 K with a series of 20 pulses (0.941 cm^3) of a mixture of 4.78% of H_2 in Ar. A stoichiometry of $H/Rh_s = 1$ was

Table 1
Dip coating procedure

Step	Conditions
Powder drying	T = 120 °C overnight
Slurry preparation	H_2O/powder = 1.7 g/g
	HNO_3/powder = 1.7 mmol/g (Rh/α-Al_2O_3)
	HNO_3/powder = 1.0 mmol/g (Rh/ZrO_2)
Ball milling	24 h with ZrO_2 spheres, 100 rpm
Dip-coating	Deposition of a primer (Disperal®), dipping, extraction at 8 cm/min
Flash drying	T = 280 °C for 10 min

assumed [27]. Very high dispersions were measured over the fresh catalysts: 60% for Rh/α-Al_2O_3 and 70% for Rh/ZrO_2.

2.2. Annular reactor

Reaction tests were carried out in a structured annular reactor, schematically drawn in Fig. 1. The annular reactor consisted of an inner catalyst-coated ceramic tube, coaxially inserted into an outer quartz tube, giving rise to an annular duct through which the gas flows in laminar regime. Negligible pressure drop were observed even at very high space velocities. Based on the predictions of a 1D model [28], the reactor was designed and the range of space velocities were chosen to reduce the importance of mass transfer limitations and to operate far from equilibrium conditions, thus extending the useful temperature range for the kinetic investigation. An annular reactor was thus realized with a channel height as thin as 0.5 mm.

Temperature profiles were measured by sliding a thermocouple inside the internal ceramic tube. Given the thermal equilibrium across the section of the ceramic tube, the measurements exactly correspond to the temperature on the catalyst surface [20]. Effective dissipation of the heat of reaction by radiation allowed to realize tests under rich conditions at the expense of acceptable thermal axial gradients if compared with those obtained in packed-bed reactors.

2.3. Reaction conditions

Tests were performed at atmospheric pressure. In standard tests diluted mixtures were fed at gas hourly space velocity (GHSV) of 1.1×10^6 l/kg_{cat}/h (NTP), with composition CH_4 = 4% (v/v), O_2/CH_4 = 0.56, N_2 to balance. This feed composition correspond to a dilution factor, Φ, of 5.8, being Φ defined as the ratio between the flow of diluting N_2 and the flow of methane and air. The slight excess of oxygen with respect to the stoichiometric value for partial oxidation helped avoiding coke formation, which was never observed in the experiments. The effect of temperature was investigated in the range 320–900 °C; space velocities varied from 1.1×10^6 l/kg_{cat}/h (NTP) to 10^7 l/kg_{cat}/h (NTP). The effects of feed dilution, with Φ varying in the range 0–5.8, and of O_2/CH_4 ratio in the range 0.56–1 were also studied.

Blank experiments verified that homogeneous reactions did not occur under these conditions. In every reaction test, the first set point temperature (about 300 °C) was achieved by a ramp of 5 °C/min to avoid dangerous thermal shocks on the alumina tube. Temperature was progressively increased up to 900 °C by increments of 10–50 °C. The inlet and outlet gas compositions were measured by a micro-GC (3000A by Agilent Technologies). At each temperature, conversions and selectivities were estimated by repeated analyses, showing stable performances within 15–20 min.

Aged catalyst samples were obtained by exposing powders of the dried slurry to standard reaction conditions, at T = 900 °C for 8 h in a packed bed reactor.

3. Results

3.1. Conditioning

The performance of the Rh-supported catalysts changed significantly after exposure to reaction conditions. Successive activation runs at standard feed composition and GHSV,

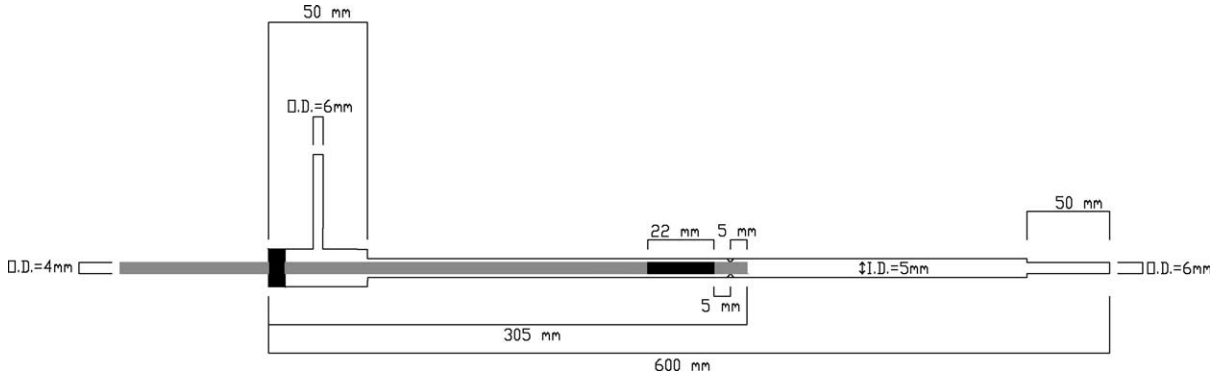

Fig. 1. Annular reactor for the study of methane partial oxidation.

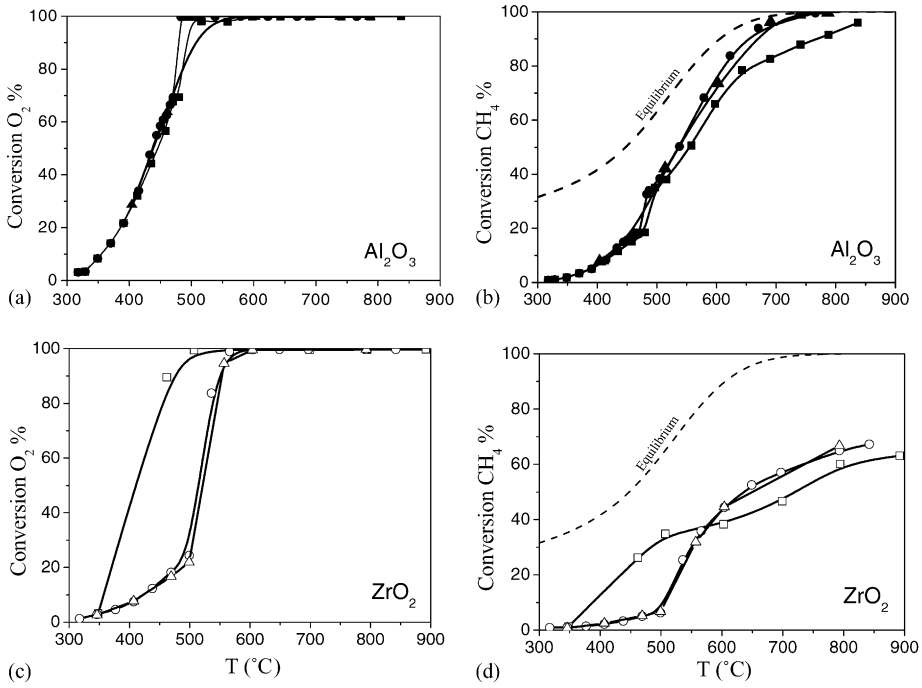

Fig. 2. Catalyst conditioning. Effect of temperature on O_2 conversion (a) and CH_4 conversion (b) for 0.5% Rh/α-Al_2O_3 ((■) 1° run; (●) 2° run; (▲) 3° run); effect of temperature on O_2 conversion (c) and CH_4 conversion (d) for 0.5% Rh/ZrO_2 ((□) 1° run; (○) 2° run; (△) 3° run). Operating conditions: P = 1.1 atm; GHSV= 1.1 × 10^6 l/kg_{cat}/h (NTP); CH_4=4%; O_2/CH_4 = 0.56, N_2 to balance (Φ = 5.8).

performed between 300 and 900 °C according to the above described procedure, were necessary to obtain a stable behavior for both catalysts. In Fig. 2, O_2 and CH_4 conversions are plotted as functions of the outlet catalyst temperature, in order to compare experimental results with calculated equilibrium values (dashed lines). As illustrated in the following, outlet temperatures were always representative of the average catalyst temperature.

3.1.1. *Rh/α-Al_2O_3*

The conditioning of Rh/α-Al_2O_3 is reported in Fig. 2a and b. Reaction first initiated at about 350 °C and the increase of temperature resulted in a sharp increase of O_2 conversion, which was complete at about 470 °C. Methane conversion increased more gradually, even after complete O_2 consumption (temperatures higher than 450 °C). The values of O_2 conversion kept unchanged after repeating the experiments; methane conversion also did not vary at the lower temperatures, but it improved considerably in the medium to high temperature range, where the production of CO and H_2 occurred.

This behavior was repeatedly observed with different catalyst batches, prepared and tested to verify the reproducibility of results. Recent experiments over Rh/Al_2O_3 catalysts prepared by using $Rh(NO_3)_3$ as metal precursor (data are omitted for the sake of brevity), indicated that the introduction of reducing pretreatments in a H_2 containing stream either at medium temperature (500 °C) or high temperature (800 °C) did not accelerate the catalyst conditioning, which suggests that the conditioning process involves a more complex transformation of the surface than the simple reduction of Rh.

3.1.2. *Rh/ZrO_2*

In the case of the Rh/ZrO_2 catalyst, changes of the catalyst behavior with time on stream were more evident, as shown in Fig. 2c and d. The initial activity of the catalyst clearly decreased in the range of low temperatures, were only CO_2 and H_2O were formed according to total combustion stoichiometry. An enhancement of methane conversion was instead observed at high temperatures, in correspondence with synthesis gas production.

3.2. *Effect of temperature*

Fig. 3 compares the performances of the two catalysts under standard operating conditions (O_2/CH_4 = 0.56, Φ = 5.8) after reach of stable behavior. O_2 and CH_4 conversion, H-atom selectivity of H_2 and C-atom selectivity of CO are plotted as functions of the outlet catalyst temperature, in order to compare experimental results with calculated equilibrium values (dashed lines).

3.2.1. *Rh/α-Al_2O_3*

The realization of a high space velocity allowed to measure intermediate O_2 conversions within a wide range of temperatures up to 470 °C. Above this temperature, a little increase of the furnace set point temperature caused a steep increase in O_2 conversion from 70% to complete consumption. Below 470 °C CH_4 conversion paralleled O_2 conver-

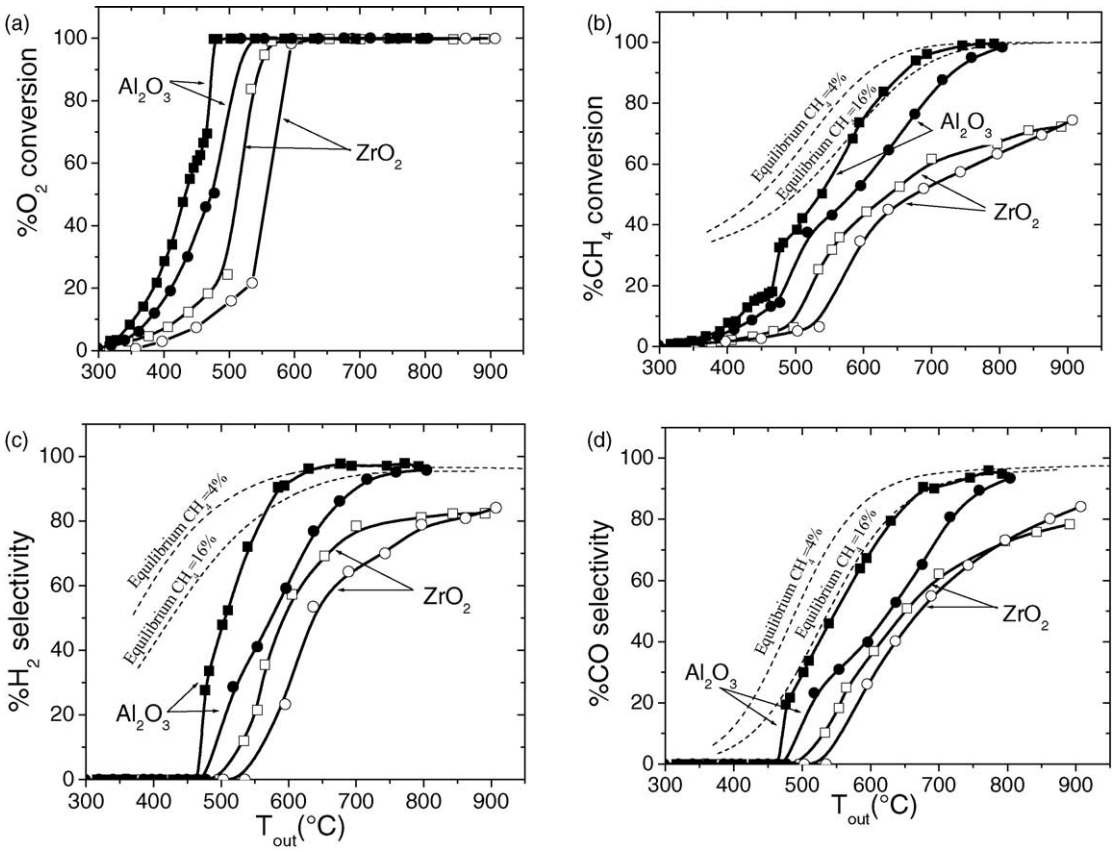

Fig. 3. Effect of dilution on O_2 conversion (a), CH_4 conversion (b), H_2 selectivity (c) and CO selectivity (d) over 0.5% Rh/α-Al_2O_3 and 0.5% Rh/ZrO_2 catalysts. Operating conditions: P = 1.1 atm; O_2/CH_4 = 0.56; GHSV = 1.1×10^6 l/kg_{cat}/h (NTP) ((■, □) Φ = 5.8 (4% CH_4); (●, ○) Φ = 0.7 (16% CH_4); (■, ●) Rh/α-Al_2O_3; (□, ○) Rh/ZrO_2).

sion according to the stoichiometry of total oxidation; at 470 °C it also showed a steep increase and then further increased with temperature, thus suggesting the existence of secondary reactions not involving oxygen. Methane conversion approached the equilibrium values at about 750 °C.

Concerning the product composition, H_2O and CO_2 were the only reaction products at low temperature and incomplete O_2 conversions. Their molar fraction passed through a maximum at 470 °C; above this temperature, in fact, H_2 and CO were formed and their selectivity steadily grew with temperature. At about 500 °C the H_2/CO ratio reached a maximum equal to 3 (the expected stoichiometry of methane steam reforming); with increasing temperature the relative production of H_2 and CO changed as the H_2/CO ratio lowered toward 2, the expected value for partial oxidation. The coexistence of several reaction stoichiometries could explain this effect.

3.2.2. Rh/ZrO_2

At stable conditions, similar trends were observed on the zirconia-based catalyst if compared with the alumina-based catalyst, although with a lower activity. Lower values of O_2 and methane conversions and smoother increases with temperatures were in fact observed; complete O_2 consumption was reached above 500 °C, but methane conversion was always below the equilibrium at all temperatures. The initial production of H_2 and CO was observed when approaching the total consumption of oxygen and was accordingly shifted to higher temperatures than over α-Al_2O_3. H_2/CO ratio was not constant with temperature, again suggesting the combined effect of several reactions: it reached a maximum of 3 at about 600 °C, then decreased to 2 with increasing temperature.

3.3. Effect of dilution

The performances of the two systems were compared at varying partial pressure of reactants, maintaining O_2/CH_4 = 0.56. Four conditions were explored: Φ = 0 (methane + air); 0.7; 2.4; 5.8 (standard conditions). Fig. 3 reports the results obtained at Φ = 0.7 and 5.8 (CH_4 = 16%, 4%, respectively).

3.3.1. $Rh/\alpha\text{-}Al_2O_3$

The decrease of Φ was accompanied by a decrease of O_2 and CH_4 conversions. In the range of low to medium temperatures, this effect was likely controlled by the process kinetics since conversions were significantly below the equilibrium. By comparing the net values of CH_4 and O_2 converted moles, it was verified that the decrease of

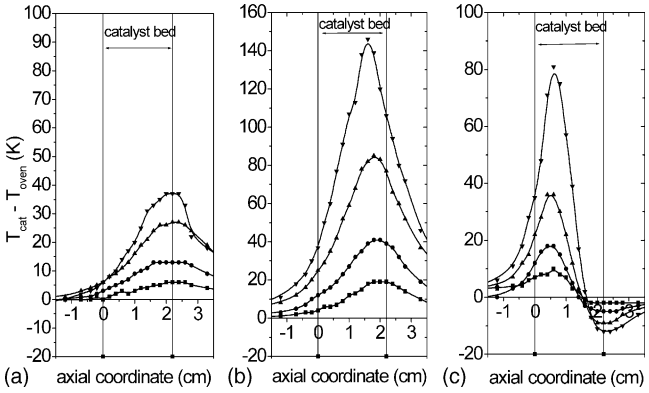

Fig. 4. Effect of dilution on temperature profiles in the reactor at three levels of CH_4 conversion (a) 8% CH_4 conversion; (b) 40% CH_4 conversion; (c) 95% CH_4 conversion); over 0.5% Rh/α-Al_2O_3 catalyst. Operating conditions: $P = 1.1$ atm; $O_2/CH_4 = 0.56$; GHSV = 1.1×10^6 l/kg_{cat}/h (NTP) ((■) $\Phi = 5.8$; (●) $\Phi = 2.4$; (▲) $\Phi = 0.7$; (▼) $\Phi = 0$).

conversion corresponded to an overall kinetic order lower than 1 in the whole temperature range. At the highest temperatures, thermodynamics might have contributed, given the negative dependence of CH_4 conversion at equilibrium upon increase of reactants partial pressure. The selectivity of H_2 and CO both decreased.

3.3.2. Rh/ZrO_2

Similarly to Rh/α-Al_2O_3, by decreasing the dilution from $\Phi = 5.8$ to 0.7, O_2 conversion decreased at low temperature; its complete consumption was shifted up of about 40 °C, which in turn delayed the curves of H_2 and CO selectivity. After reach of complete O_2 conversion, however, the effect of Φ on methane conversion and synthesis gas production was clearly less important than on the alumina-supported catalyst.

3.3.3. Temperature-profiles

The effect of temperature and of dilution on the axial temperature profile is shown in Fig. 4, for the alumina-based catalyst. The panels refer to three different levels of CH_4 conversion, 8%, 40% and 95%, representative of three characteristic cases: the low temperature region wherein a highly exothermic process as deep methane oxidation proceeded, the intermediate temperature region (the mostly severe one) wherein O_2 conversion completed and exothermicity was at a maximum due to high selectivity to CO_2 and H_2O, the high temperature region wherein H_2 and CO prevailed in the product mixture. Temperature profiles were characterized by the presence of an hot-spot differently located along the catalyst according to the temperature: at low temperature the maximum established at the exit of the catalyst layer, but with increasing temperature the hot spot moved back toward the initial catalyst section. At the highest temperatures a maximum at the very beginning of the catalyst bed was followed by a minimum (see Fig. 4c, CH_4 conversion 95%). With decreasing dilution, maxima and minima became more evident. Such profiles represent the evidence of the occurrence of exothermic reactions in the O_2 rich zone at the catalyst bed inlet, followed by endothermic reactions in the O_2 depleted zone at the catalyst bed outlet.

Axial gradients were considerably lower than those characteristic of traditional packed-bed reactors. Note that at high dilution ($\Phi = 5.8$) maximum ΔT along the catalyst bed kept below 10 °C under all the investigated conditions, which can afford an "isothermal" kinetic analysis of the experimental data.

On zirconia-based catalyst, the effect of dilution (not shown) on axial temperature profile was qualitatively the same, even if there was no evidence of a minimum, in line with a lower activity to syngas production at high temperature.

3.4. Effect of space velocity

GHSV was increased from 1.1×10^6 l/kg_{cat}/h (NTP) to 3.4×10^6 l/kg_{cat}/h (NTP) and to 10^7 l/kg_{cat}/h (NTP), by increasing the total flow rate at standard feed composition. Selected results are reported in Fig. 5 and compared with calculated trends at equilibrium (dashed lines).

3.4.1. $Rh/\alpha\text{-}Al_2O_3$

In the case of the alumina-based system, the conversions of both reactants decreased significantly at increasing space velocity; at 10^7 l/kg_{cat}/h (NTP) the process was far from thermodynamic equilibrium even at high temperatures. O_2 conversion did not reach 100%; at high temperatures the experimental curve flattened, likely due to mass transfer limitations. In fact, an apparent activation energy of nearly 85 kJ/mol was estimated at temperatures lower than 550 °C in line with the existence of a chemical regime, but it decreased to 28 kJ/mol at higher temperatures, thus suggesting the existence of a mixed chemical-diffusion regime.

Syngas production was strongly influenced by contact time. With increasing GHSV, H_2 and CO selectivities lowered, according to the behavior of secondary products in a consecutive scheme. Besides, H_2 selectivity decreased more significantly than CO selectivity, which resulted in the net decrease of the H_2/CO ratio with increasing GHSV. The dependence of H_2/CO ratio on both temperature and GHSV is an evidence that more than one reaction (thus several combined stoichiometries) were involved in the production/consumption of H_2 and CO.

3.4.2. Rh/ZrO_2

Also in the case of the zirconia-based system, O_2 and CH_4 conversions decreased with increasing GHSV, as expected. As a further evidence in favor of the lower activity of this catalyst with respect to the alumina-based one, at GHSV = 10^7 l/kg_{cat}/h (NTP), the measured trend of O_2 conversion was very smooth. The apparent activation energy was estimated at ≈74 kJ/mol below 800 °C, a sufficiently

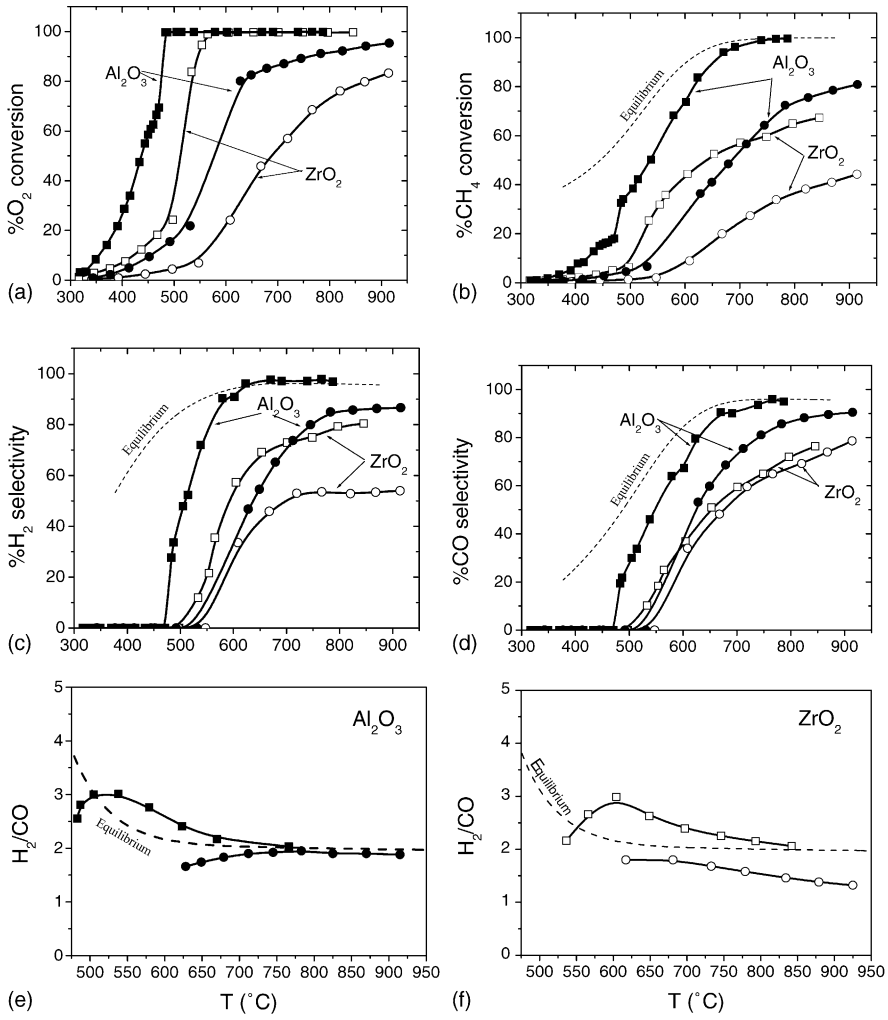

Fig. 5. Effect of space velocity on O_2 conversion (a), CH_4 conversion (b), H_2 selectivity (c), CO selectivity (d) and H_2/CO ratio (e) and (f) over 0.5% Rh/α-Al_2O_3 and 0.5% Rh/ZrO_2 catalysts. Feed composition as in Fig. 2 ((■, □) GHSV = 1.1 × 10^6 l/kg_{cat}/h (NTP); (●, ○) GHSV = 10 × 10^6 l/kg_{cat}/h (NTP)).

high value to consider the process under chemical regime; at higher temperatures, a mixed chemical diffusion regime prevailed. Concerning the product distribution, H_2 selectivity was negatively affected by the increase of space velocity; instead, CO selectivity was rather unaffected by GHSV. As a result, the H_2/CO ratio, which was close to 2 at low GHSV, progressively lowered at high space velocity with increasing temperature. Still, it is remarkable that, though in the presence of residual O_2, synthesis gas production was significant; this could be interpreted as an evidence in favor of a direct route to CO and H_2.

3.5. Effect of oxygen to methane ratio

At standard GHSV of 1.1 × 10^6 l/kg_{cat}/h (NTP), the effect of oxygen partial pressure was investigated by varying the O_2/CH_4 ratio from 0.56 to 1, while maintaining CH_4 concentration at 4%. Fig. 6 compares the results observed in the cases of O_2/CH_4 = 0.56 and 1.

3.5.1. Rh/α-Al_2O_3

In the range of low temperatures, where methane combustion was the unique process, O_2 conversion decreased markedly upon increase of the O_2/CH_4 ratio, while CH_4 conversion was unaffected. Also, the increase of O_2 partial pressure enlarged the region of deep oxidation, thus delaying significantly the onset of those reactions which formed H_2 and CO. A shift to higher temperatures of the selectivity curves was in fact evident. When oxygen conversion was complete, than methane conversion registered a steep increase leading to higher values than those measured at O_2/CH_4 = 0.56, as predicted by thermodynamics.

3.5.2. Rh/ZrO_2

Also over the zirconia-based catalyst, low temperature O_2 conversion decreased while methane conversion kept unchanged with increasing O_2/CH_4 ratio. Again the increase of O_2 concentration resulted in a significant shift to higher

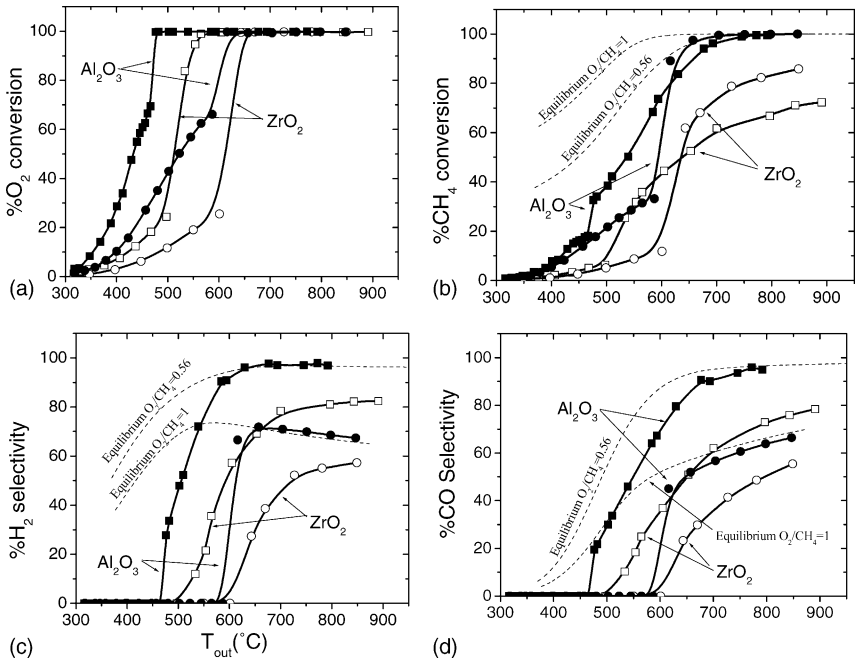

Fig. 6. Effect of oxygen to methane ratio on O_2 conversion (a), CH_4 conversion (b), H_2 selectivity (c) and CO selectivity (d) over 0.5% Rh/α-Al_2O_3 and 0.5% Rh/ZrO_2 catalysts. Operating conditions: $P = 1.1$ atm; $CH_4 = 4\%$; GHSV = 1.1×10^6 l/kg_{cat}/h (NTP) ((■, □) $O_2/CH_4 = 0.56$; (●, ○) $O_2/CH_4 = 1$).

temperature of the reactions responsible for H_2 and CO formation. Also in this case, when oxygen was completely consumed, methane conversion definitely increased. Then, at high temperature the curve of methane conversion relating to $O_2/CH_4 = 1$ crossed the corresponding curve at $O_2/CH_4 = 0.56$, reflecting the thermodynamic trends; still, the higher conversion values were lower than the equilibrium ones.

4. Discussion

The operating conditions realized in the annular reactor allowed to perform activity tests under a kinetic controlled regime. The adoption of a narrow channel opening and the deposition of thin catalyst layers minimized and confined to high temperatures the effect of interphase and intraporous mass transfer limitations. By feeding high flow rates and loading small catalyst amounts, space velocity could be varied between 10^6 and 10^7 l/kg_{cat}/h (NTP), which allowed to skip the thermodynamic control and measure values of methane and O_2 conversions below the equilibrium values. Most important, the catalyst temperature could be measured directly from inside the catalyst tubular support and almost isothermal conditions were guaranteed by the radiative heat dispersion from the catalyst layer. All these favorable features, hardly achievable with standard packed bed reactors or autothermal structured reactors, provided the tool for evidencing kinetic effects of methane partial oxidation over 0.5% Rh/α-Al_2O_3 and 0.5% Rh/ZrO_2 catalysts.

It was found that, once exposed to the reaction conditions, the performaces of the Rh-supported catalysts slowly changed. Several hours at standard conditions were necessary over both the fresh catalysts to obtain a stable activity. On Rh/α-Al_2O_3, the low temperature activity (that is the activity of the oxidation reactions) kept unchanged during conditioning; instead, the high temperature activity (that is the activity responsible for CO/H_2 formation) improved considerably with time on stream. In the case of the Rh/ZrO_2 catalyst, instead, the initial high oxidation activity was partly suppressed with time; similarly to α-Al_2O_3, an enhancement of the activity of secondary reactions was observed at high temperatures.

The activation process suggested that modifications of the superficial structure of the catalysts must have occurred, probably the result of combined effects, such as the exposure to high temperature and to a complex reacting mixture. Notably, in both cases, catalyst conditioning seemed to preserve Rh dispersion: over aged catalysts it amounted to 35% for 0.5% Rh/α-Al_2O_3 and to 48% for 0.5% Rh/ZrO_2. TEM images, not reported, on both fresh and aged samples after exposure at reaction conditions also showed that severe sintering effects did not happen as Rh aggregates kept an average size of about 20 Å. Besides, experiments over a Rh/α-Al_2O_3 catalyst prepared by using $Rh(NO_3)_3$ as metal precursor showed that the conditioning process is not a simple reduction process. A reconstruction of Rh aggregates might explain the modification of the catalytic behavior in spite of the unaffected Rh morphology, which deserves further investigation.

Concerning the steady-state performances of the 0.5% $Rh/\alpha\text{-}Al_2O_3$, an extremely high activity for syngas production was observed: the conversion of O_2 and CH_4, the selectivity of H_2 and CO reached the equilibrium values at $T < 800\ ^\circ C$. In line with the findings of other authors over Rh-supported catalysts [11], CO_2 and H_2O were uniquely observed at the lower temperatures where the process initiated; H_2 and CO were instead high temperature products and the highest selectivities were observed in correspondence with complete oxygen consumption. The dependences of conversions and product distribution on the reaction temperature suggested that the most probable reaction scheme for syngas formation was an indirect scheme: H_2 and CO mainly formed through the secondary reactions of steam and CO_2 reforming of methane, driven by the primary deep oxidation of methane. In line with the existence of secondary endothermic reactions, the shape of the axial temperature profiles always showed a maximum at the very beginning of the catalyst bed followed by a gradual temperature decrease, and even a minimum at the highest temperatures. A further evidence of an indirect mechanism of formation of syngas was observed by reducing the contact time. In fact, an increase of space velocity lowered not only O_2 and CH_4 conversions, but also H_2 and CO selectivities. These observations are in line with the those reported by several authors, who proposed an indirect reaction scheme for methane partial oxidation over noble metal-supported catalysts [29–31] and specifically over Rh-supported catalysts [13,32].

The present data, however, provided evidence that the formation of CO and H_2 proceeds through a more complex path than a simple consecutive combustion/reforming scheme. Considering the H_2/CO ratio, in fact, it showed dependencies from temperature and GHSV. At standard GHSV and increasing temperature (complete O_2 conversion), the H_2/CO ratio passed through an initial maximum of 3 (characteristic of the steam reforming stoichiometry) and decreased to 2 at high temperature. This trend can be explained by the combined effect of steam reforming, dry reforming and water gas shift. The latter reaction closely approached the equilibrium at high temperatures, thus WGS may have provided a path of reorganization between CO, H_2O, H_2 and CO_2 which contributed to lower the high temperature H_2/CO ratio to 2. Concerning the effect of GHSV, at high space velocity (and lower O_2 conversions) the H_2/CO ratio decreased over both catalysts. Analogous results were independently observed in a previous work [28]; there, it was verified that the decrease of H_2/CO ratio observed on a Rh/alumina catalyst with increasing space velocity could be quantitatively explained by an indirect-consecutive scheme, that is by assuming that H_2 and CO underwent consecutive oxidations to H_2O and CO_2.

Hypothesizing that H_2 combustion was much faster than CO combustion, which was verified by preliminary experiments herein not reported, such consecutive reactions could explain the lowering of the H_2/CO ratio in the presence of residual amount of O_2 at low temperature and high GHSV.

Many qualitative analogies could be recognized between the 0.5% Rh/ZrO_2 and 0.5% $Rh/\alpha\text{-}Al_2O_3$ systems. Over Rh/ZrO_2, at lower space velocity, the observed trends were largely in line with those obtained over $Rh/\alpha\text{-}Al_2O_3$. An indirect kinetic scheme apparently prevailed. However, at high space velocity H_2 and CO yields markedly decreased, but were still important though O_2 conversion was not complete. Notably, due to the lower oxidation activity, the process was not strongly mass-transfer limited (as in the case of the alumina-based catalyst) and the catalyst surface must have experienced significant values of O_2 concentration at all temperatures. This behavior could suggest the presence of a direct reaction of partial oxidation.

At increasing space velocity, the decrease of H_2/CO ratio was even more evident than over the Rh-alumina catalyst. This could be explained by a major role of consecutive H_2 and CO oxidations due to the larger amount of residual oxygen which resulted from the lower rate of methane combustion; still, an additional partial oxidation route (expected $H_2/CO = 2$) may have played an important role.

Along the line of an indirect-consecutive scheme, the behaviour observed during conditioning suggested that at least two types of active sites, responsible for oxidation and reforming reactions, respectively, coexisted on the surface of the Rh-supported catalysts.

A preliminary kinetic analysis was performed investigating the effects of partial pressure of reactants and of O_2/CH_4 ratio. Over both catalysts, the kinetics of methane total oxidation, occurring in the range of low temperatures (350–500 °C), was practically independent on O_2 partial pressure and showed an overall reaction order lower than 1 upon decreasing dilution. This effect could be explained by assuming a first order dependence on CH_4, and the existence of an inhibiting effect from adsorption of reaction products (likely H_2O). Remarkably, O_2 adsorption showed a strong inhibiting effect on the rate of secondary reactions: on both catalysts, the increase of O_2 partial pressure shifted to higher temperatures the onset of steam and CO_2 reforming and the production of CO and H_2.

5. Conclusion

An annular reactor characterized by narrow channel opening and thin catalyst layers, operating at extremely high values of space velocity far from thermodynamic equilibrium allowed to evidence several kinetic aspects of methane partial oxidation over Rh-supported catalysts, so far unreported in the technical literature.

Evolution of the performances of the fresh catalysts under reaction conditions, with specific activation of the high temperature reactions responsible of syngas production, suggested the probable occurrence of reduction and reconstruction of the Rh aggregates. This in turn implies

the key role of the conditioning procedure in determining the final catalyst performances.

The analysis of the effects of temperature, space velocity, feed composition as well as the shape of temperature profiles indicated that methane partial oxidation over $Rh/\alpha\text{-}Al_2O_3$ and Rh/ZrO_2 mainly proceeded according to an indirect-consecutive scheme, consisting of methane deep oxidation, methane steam and dry reforming, WGS and H_2 and CO oxidations. However, in the case of Rh/ZrO_2, significant H_2 yields were observed at high space velocity in the presence of unconverted O_2 and the possible contribution of a direct route to synthesis gas could not be excluded. The rationalization of these evidences needs the means of the theoretical analysis, which is expected to provide a quantitative estimate of the rates of the single reactions on the different catalysts.

Acknowledgement

The financial supports from MIUR-Roma, EU Cathlean Project and NEMAS (Nano Engineered Materials and Surfaces) are gratefully acknowledged.

Reference

[1] D.A. Hickman, E.A. Haupfear, L.D. Schmidt, Catal. Lett. 17 (1993) 223.
[2] K.L. Hohn, L.D. Schmidt, Appl. Catal. A: Gen. 211 (2001) 53.
[3] C.A. Leclerc, J.M. Redenius, L.D. Schmidt, Catal. Lett. 79 (2002) 39.
[4] K.H. Hofstad, J.H.B.J. Hoebink, A. Holmen, G.B. Marin, Catal. Today 40 (1998) 157.
[5] O.V. Buyevskaya, K. Walter, D. Wolf, M. Baerns, Catal. Lett. 38 (1996) 81.
[6] L. Basini, K. Aasberg-Petersen, A. Guarinoni, M. Østberg, Catal. Today 64 (2001) 9.
[7] F. Basile, G. Fornasari, M. Gazzano, A. Kiennemann, A. Vaccari, J. Catal. 217 (2003) 245.
[8] J.N. Armor, Appl. Catal. A: Gen. 179 (1999) 159.
[9] H. Karim, K. Lyle, S. Etemad, L. Smith, W. Pfefferle, P. Dutta, K. Smith, ASME Paper GT-2002-30083.
[10] J. Zizelman, S. Shaffer, S. Mukerjee, SAE Technical Paper 2002-01-0411.
[11] P. Aghalayam, Y.K. Park, D.G. Vlachos, Catalysis 15 (2000) 98.
[12] A.S. Bodke, S.S. Bharadwaj, L.D. Schmidt, J. Catal. 179 (1998) 138.
[13] Y. Boucouvalas, Z. Zhang, X.E. Verykios, Catal. Lett. 40 (1996) 189.
[14] E. Ruckenstein, H.Y. Wang, J. Catal. 187 (1999) 151.
[15] L. Majocchi, G. Groppi, C. Cristiani, P. Forzatti, L. Basini, A. Guarinoni, Catal. Lett. 65 (2000) 49.
[16] D. Wang, O. Dewaele, A.M. De Groote, G.F. Froment, J. Catal. 159 (1996) 418.
[17] Y. Boucouvalas, Z. Zhang, X.E. Verykios, Catal. Lett. 27 (1994) 131.
[18] I. Tavazzi, A. Beretta, G. Groppi, P. Forzatti, in: Proceedings of the DGMK Conference Innovation in the Manufacture and Use of Hydrogen, Dresden, October 15–17, 2003.
[19] G. Groppi, W. Ibashi, E. Tronconi, P. Forzatti, Chem. Eng. J. 82 (2001) 57.
[20] W. Ibashi, G. Groppi, P. Forzatti, Catal. Today 83 (2003) 115.
[21] A. Beretta, P. Forzatti, J. Catal. 200 (2001) 45.
[22] L. Basini, M. Marchionna, S. Rossini, D. Sanfilippo, US Patent 5,336,655 (1994).
[23] L.L.G. Jacobs, P.W. Lednor, A.G.G. Limahelu, R.J. Schoonebeek, K.A. Vonkeman, US Patent, 5,510,056 (1996).
[24] C. Wong, R.W. McCabe, J. Catal. 119 (1989) 47.
[25] L. Basini, M. Marchionna, A. Aragno, J. Phys. Chem. 96 (1992) 9431.
[26] K. Pokrovski, K.T. Jung, A.T. Bell, Langmuir 17 (2001) 4297.
[27] J.R. Anderson, K.C. Pratt, Introduction to Characterization and Testing of Catalysts, Academic Press, Australia, 1985.
[28] I. Tavazzi, A. Beretta, G. Groppi, P. Forzatti, Stud. Surf. Sci. Catal. VII Nat. Gas Convers. 147 (2004) 163.
[29] M. Prettre, C. Eichner, M. Perrin, Trans. Faraday Soc. 42 (1946) 335.
[30] P.D.F. Vernon, M.L.H. Green, A.K. Cheethan, A.T. Ashcroft, Catal. Lett. 6 (1990) 181.
[31] F. van Looij, E.R. Stobbe, J.W. Geus, Catal. Lett. 50 (1998) 59.
[32] K. Heitnes Hofstad, B. Andersson, A. Holmgren, O.A. Rockstad, A. Holmen, Stud. Surf. Sci. Catal. IV Nat. Gas Convers. 107 (1997) 415.